Acta Neuropathol (1999) 98 : 493–505

REGULAR PAPER

Ethan N. Goldstein · Cheri R. Owen · Blaine C. White
José A. Rafols

Ultrastructural localization of phosphorylated eIF2α [eIF2α(P)] in rat dorsal hippocampus during reperfusion

Received: 12 February 1999 / Revised, accepted: 16 April 1999

Abstract During post-ischemic brain reperfusion there is a substantial reduction of protein synthesis in selectively vulnerable neurons. Normal protein synthesis requires a functional translation initiation complex, a key element of which is eukaryotic initiation factor 2 (eIF2), which in a complex with GTP introduces the met-tRNA$_i$. Phosphorylation of Ser^{51} on the α subunit of eIF2 [eIF2α(P)] generates a competitive inhibitor of eIF2B, thereby preventing the replenishment of GTP onto eIF2, thus blocking translation initiation. It has been shown that the conditional expression of an eIF2α mutant (Asp substituted for Ser^{51}) imitating the negative charge of Ser^{51} (P) induces apoptosis. During the first 10 min of post-ischemic reperfusion, there is an approximately 20-fold increase in eIF2α(P) seen in the cytoplasm of CA1 hippocampal neurons, and, by 1 h, there is also accumulation of eIF2α(P) in the nucleus. We utilized post-embedding electron microscopical immunogold methods to examine the localization of eIF2α(P) during reperfusion. Immunogold particles (10 nm) were concentrated chiefly along the rough endoplasmic reticulum and in association with the membranes of the nuclear envelope in CA1 neurons. Aggregations of gold particles in the nucleus were concentrated: (1) within and around the nucleolus, (2) associated to strands of heterochromatin, and (3) along putative nuclear filaments. The presence of eIF2α(P) in the nucleolus probably reflects its association with nascent ribosomal subunits. The β-subunit of eIF2 has a zinc finger and polylysine blocks analogous to those on other proteins that affect transcription. The association of eIF2α(P) with chromatin may have important implications for transcription.

Key words Ischemia · Protein synthesis · Translation · Ultrastructure · Hippocampus

E. N. Goldstein · J. A. Rafols (✉)
Department of Anatomy and Cell Biology,
Wayne State University School of Medicine,
540 E. Canfield, Detroit, MI 48201, USA
Fax: +1-313-577-4131

C. R. Owen · B. C. White
Department of Emergency Medicine,
Wayne State University School of Medicine,
Detroit, Michigan, USA

C. R. Owen · B. C. White
Department of Physiology,
Wayne State University School of Medicine,
Detroit, Michigan, USA

Introduction

The long-term effects of global brain ischemia and reperfusion are often devastating to patients. In working toward improving functional recovery after stroke or cardiac arrest, our laboratory has focused on understanding the pathophysiological mechanisms involved in brain injury caused by ischemia and reperfusion.

Reperfusion following global ischemia causes a prompt and prolonged suppression of protein synthesis in selectively vulnerable neurons (SVNs) [14] in the CA1 and hilar regions of the hippocampus and in layers III, V, and VI of the cerebral cortex [4, 22]. According to studies by Nowak et al. [12], this reduction in protein synthesis is a consequence of reperfusion, and as little as 3 min of ischemia leads to suppression of protein synthesis during reperfusion. It is now generally accepted that this reperfusion-induced depression of protein synthesis is a result of inhibition of translation initiation [3].

Translation initiation is managed by a group of proteins known as eukaryotic initiation factors (eIFs). The assembly of the initiation complex is an intricate process involving over 140 proteins and requiring at least 9 initiation factors in the eukaryotic cell [11]. Specifically, the overall rate of translation initiation is regulated by the molar relationship of eIF2α(P) to eIF2B [6, 16, 18]. eIF2 is a heterotrimeric protein containing α, β and γ subunits. Translation initiation requires that a complex formed by: (1) eIF2, (2) GTP, and (3) the initiator methionyl-tRNA (Met-tRNA$_i$) deliver Met-tRNA$_i$ to the P-site of the 43S ribosomal subunit. During translation initiation, the GTP

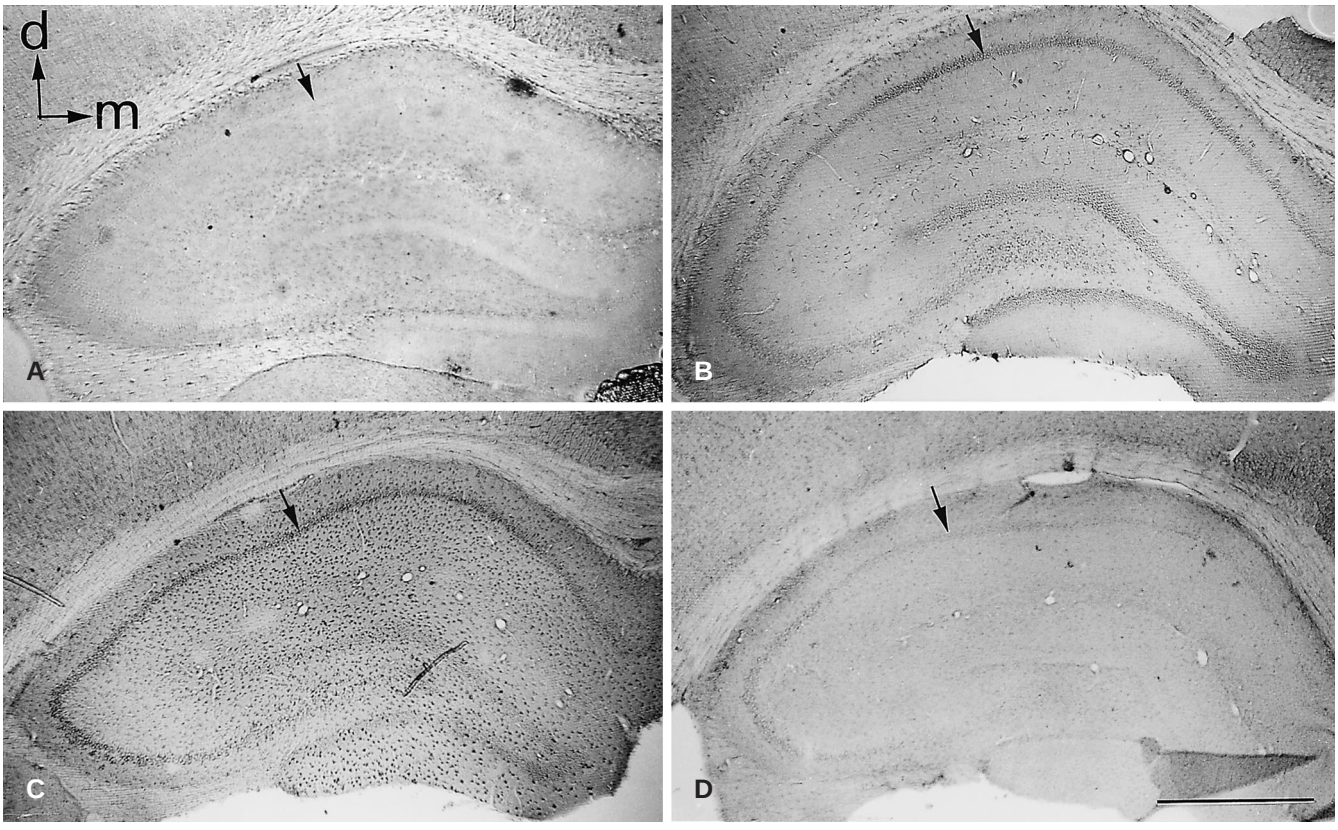

Fig. 1 A–D Photomicrographs of eIF2α(P) immunostaining in coronal sections through the dorsal hippocampus of rats. **A** Control, **B** 10-min ischemia and 10-min reperfusion, **C** 10-min ischemia and 1-h reperfusion, **D** 10-min ischemia and 10-min reperfusion with primary antibody preblocked with 55 nM antigenic peptide. Chromogen affinity of large myelinated fibers may be responsible for the nonspecific staining of the alveus. *Arrows* in all the sections point at the pyramidal cell layer of the hippocampal CA1. *Orthogonal arrows* in **A** indicate dorsal *(d)* and medial *(m)* directions. *Bar* **D** (same for all sections) 1 mm

is hydrolyzed, and the eIF2-GDP complex is released. The guanine nucleotide exchange enzyme, eIF2B, must catalyze the release of GDP from the eIF2-GDP complex to regenerate the eIF2-GTP complex before eIF2 can participate in a subsequent round of translation initiation. Phosphorylation of Ser^{51} on the α-subunit of eIF2 [eIF2α(P)] generates a tightly bound competitive inhibitor of eIF2B [6, 17]. Because the concentration of eIF2 is four to five times that of eIF2B in the brain, when approximately 20–25% of total eIF2α is phosphorylated, translation initiation is substantially inhibited.

Previous work in our laboratory identified, in brain homogenates, a reperfusion-induced approximately 25-fold increase in eIF2α(P) to more than 20% of total eIF2α, and then characterized the spatio-temporal localization of eIF2α(P) in brain coronal sections after 10 min of ischemia followed by either 10 min, 60 min, or 4 h of reperfusion [4]. This work further demonstrated that eIF2α(P) initially accumulated in the perikaryal cytoplasm of neurons, but by 1 h of reperfusion was also prominent in the nuclei of SVNs. The present investigation aimed to: (1) confirm the localization of eIF2α(P) in the reperfused rat hippocampus, and (2), for the first time, show the ultrastructural localization of eIF2α(P) in the CA1 sector during brain reperfusion.

Methods

Animal model

All animal experiments were approved by the Wayne State University Animal Investigation Committee and were conducted following the "Principles of Laboratory Animal Care" (NIH publication No. 86-23, revised in 1985). Male Long Evans rats (425–500 g) were anesthetized (44 mg/kg i.m. ketamine and 5 mg/kg i.m. xylazine), and femoral vessels were catheterized. The animals were monitored for arterial pressure, ECG, and core temperature, and were subjected to a 10-min cardiac arrest followed by resuscitation and intensive care as previously described [3].

Immunohistochemistry

Animals (n = 10; 8 experimentals and 2 non-ischemic controls) were perfused transcardially with 0.1 M phosphate buffer (PB, pH 7.4) containing 5 μM okadaic acid (to inhibit serine phosphatases [2]), followed by 250 ml fixative containing 4% paraformaldehyde and 0.1% glutaraldehyde in 0.1 M PB. Brains were removed and immersed in the same fixative overnight at 4 °C. Coronal sections, 30 μm in thickness, were prepared from non-ischemic and control brains with a vibratome and collected in 0.1 M phosphate-buffered saline (PBS, pH 7.4). Immunostaining was performed using our antibody specific to Ser^{51}-phosphorylated eIF2α [4] and the avidin-biotinylated-peroxidase complete kit (Vector Laboratories, Burlingame, Calif.). Briefly, single sections were treated with 3% hydrogen peroxide for 10 min, washed three times in PBS, perme-

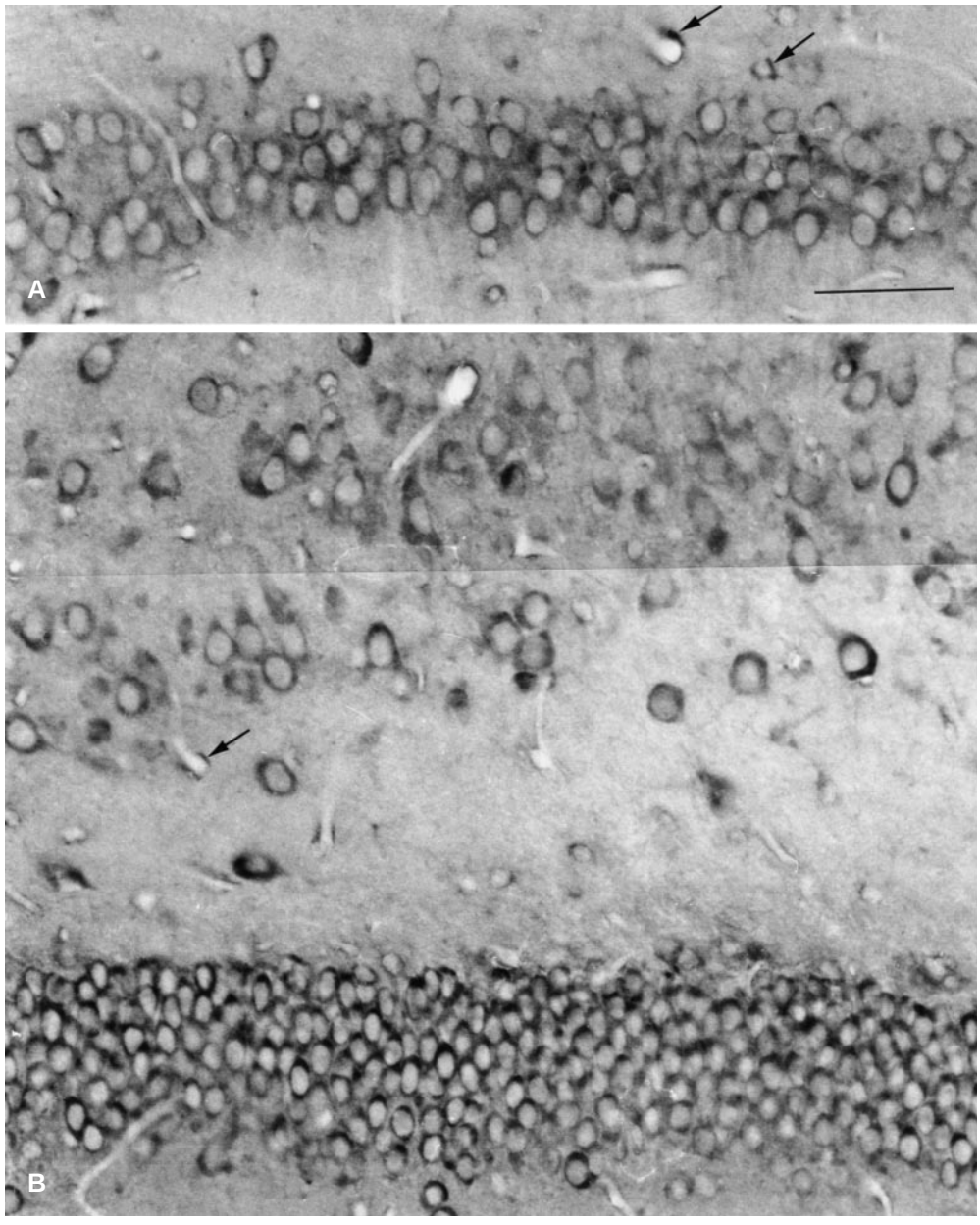

Fig. 2 A, B Immunostaining for eIF2α(P) in coronal sections through the dorsal hippocampus of a rat subjected to 10-min ischemia and 10-min reperfusion. **A** Note that CA1 immunostaining occurs primarily in the cytoplasm of pyramidal neurons. *Arrows* point at immunostaining in microvascular endothelium and in a supporting cell. **B** Photomontage including the hilar region (*upper 2/3* of figure) and the ventral blade of the dentate gyrus. *Single arrow* points at stained endothelium. *Bar* **A** (also for B) 100 μm

abilized in 0.3% Triton X-100 for 15 min, and washed three times in PBS. Tissue sections were then pretreated with 1% SDS in PBS for 5 min, rinsed in PBS, and then heated for 10 min in an 80 °C waterbath to retrieve antibody binding sites [1], preblocked in 10% goat serum for 30 min and incubated at 4 °C in anti-eIF2α(P) diluted 1 : 100 in PBS overnight. Concomitant immunostaining controls performed on adjacent sections included: (1) preblocking the primary antibody with 55 nM antigenic peptide, and (2) omitting the primary antibody. The same immunostaining controls were performed concurrently on non-ischemic brain sections. All sections were then washed three times in PBS and incubated for 1 h in the avidin-biotinylated-peroxidase complex goat anti-rabbit IgG diluted 1 : 20 in 0.15% normal goat serum and PBS. Immunoreactivity was detected using 0.03% hydrogen peroxide and 0.01% diaminobenzidine in PBS, and the reaction was terminated by washing three times with PBS.

Immunogold electron microscopy

The same brains were used to obtain 300-μm coronal sections, and the CA1 sector of the dorsal hippocampus at approximately 4 mm posterior to Bregma was microdissected. Consecutive vertical cuts were made to include a 2–3-mm width of the CA1 sector from the alveus to the dentate gyrus. This was followed by a dorsal cut longitudinal to the alveus and another longitudinal cut approximately 1 mm ventral to the alveus at the hippocampal fissure. The tissue blocks were dehydrated in increasing ethanol concentrations of 50%, 70%, 95% (3 × 5 min each), and 100% (3 × 10 min), incubated in propylene oxide (3 × 10 min) followed by 1 : 1 propylene oxide/Araldite plastic overnight, and then placed in fresh 100% Araldite plastic for 5 h, embedded in beam capsules, and polymerized for 72 h in a 60 °C oven. A Leica Ultracut microtome was utilized to obtain 0.1-μm sections, which were placed on 300 mesh gold grids. The sections were then hydrated in 0.1 M TRIS-buffered saline (TBS) for 3 min, etched in 5% sodium metaperiodate [20] (in 0.1 M TBS) for 5 min, blocked in 10% goat serum (in 0.1 M TBS) for 30 min, and placed in anti-eIF2α(P) 1 : 50 in 0.1 M

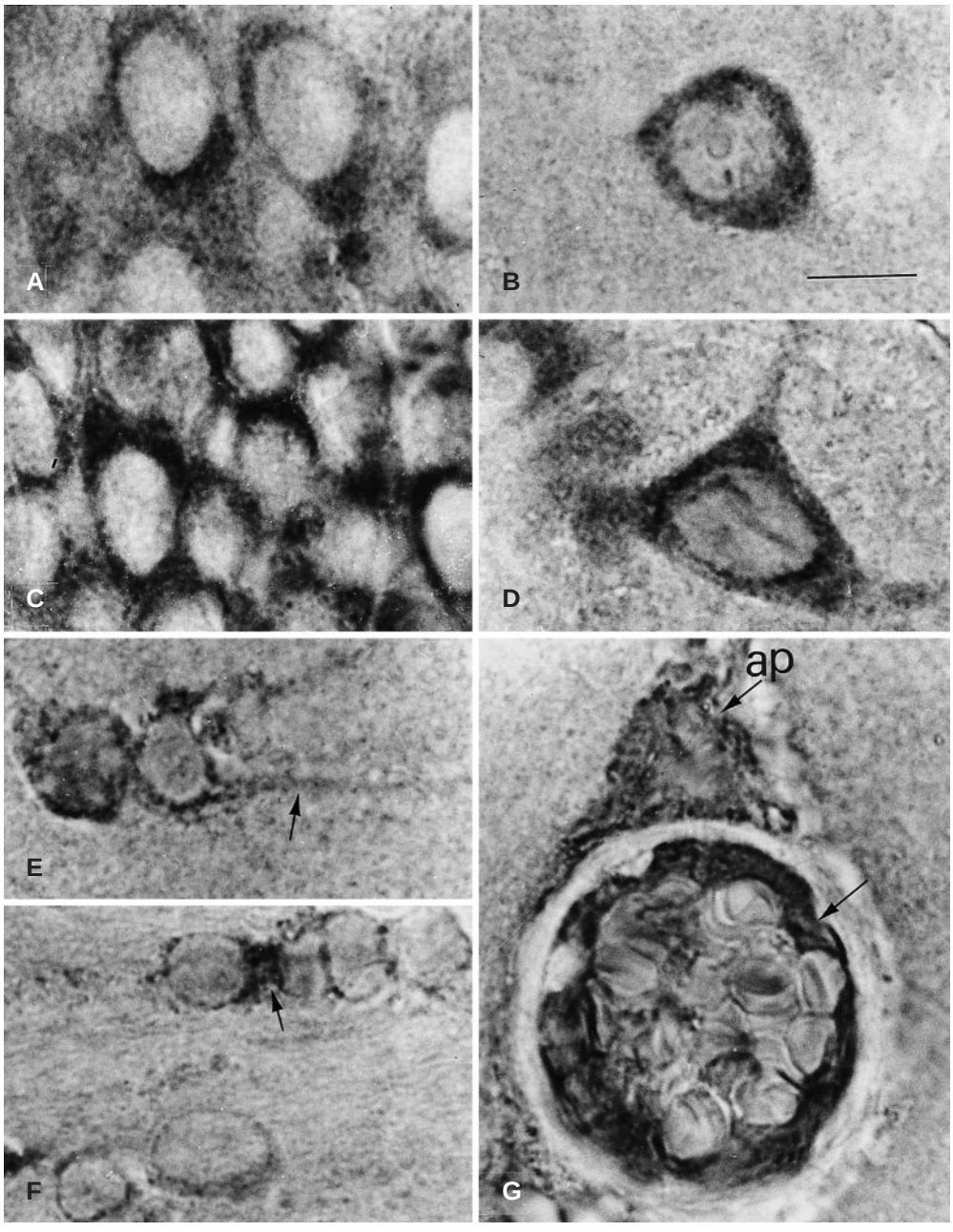

Fig. 3 A–G eIF2α(P) immunostained cells following 10-min ischemia and 10-min reperfusion. **A** Stained CA1 pyramidal neurons. **B** Stained interneuron in the CA1 stratum oriens. **C** Stained granule cells in the ventral blade of the dentate gyrus. **D** Stained hilar cell. **E** Two lightly stained astrocytes in the CA1 molecular layer; *arrow* indicates immunostained astrocytic process. **F** Corpus callosum. *Arrow* points at the stained cytoplasm of an interfascicular oligodendrocyte. **G** *Arrow* points at deep staining in the endothelial layer of a hippocampal arteriole. A large astrocytic foot process *(ap)* apposed to the vessel is lightly stained. Note that the arterial smooth muscle layer, between the endothelium and the perivascular sheath, is unstained. *Bar* **B** (also for **A, C–G**) 10 μm

TBS overnight. Grids were then rinsed 3 times in TBS and placed in 1 : 40 10-nm gold-conjugated goat anti-rabbit IgG in 0.1 M TBS for 2 h, rinsed 3 times in TBS and 20 times in dH_2O. Finally, grids were stained with uranyl acetate and lead citrate and visualized using a JEOL 1010 electron microscope. Ten neuronal cell body profiles in the pyramidal cell layer from each CA1 sector were analyzed for the presence of immunogold (IG) particles. Although no quantitative analyses were carried out, the qualitative numbers and distributions of IG particles in all the cell body profiles observed for either time of reperfusion were consistently similar. Hippocampal blood vessel lumina from both control and experimental brains were analyzed to determine background levels of IG particles.

Results

Pattern of eIF2α(P) immunostaining in dorsal hippocampus

Characteristic patterns of eIF2α(P) immunostaining that contrasted with those from controls were observed in single coronal sections through the dorsal hippocampus of rat brains subjected to ischemia and reperfusion. At low magnification very little staining was observed in sections from non-ischemic rat brains (Fig. 1 A), whereas intense staining was present in sections from brains subjected to 10-min ischemia and 10-min (Fig. 1 B) and 60-min (Fig. 1 C) reperfusion, respectively. In contrast, no immunola-

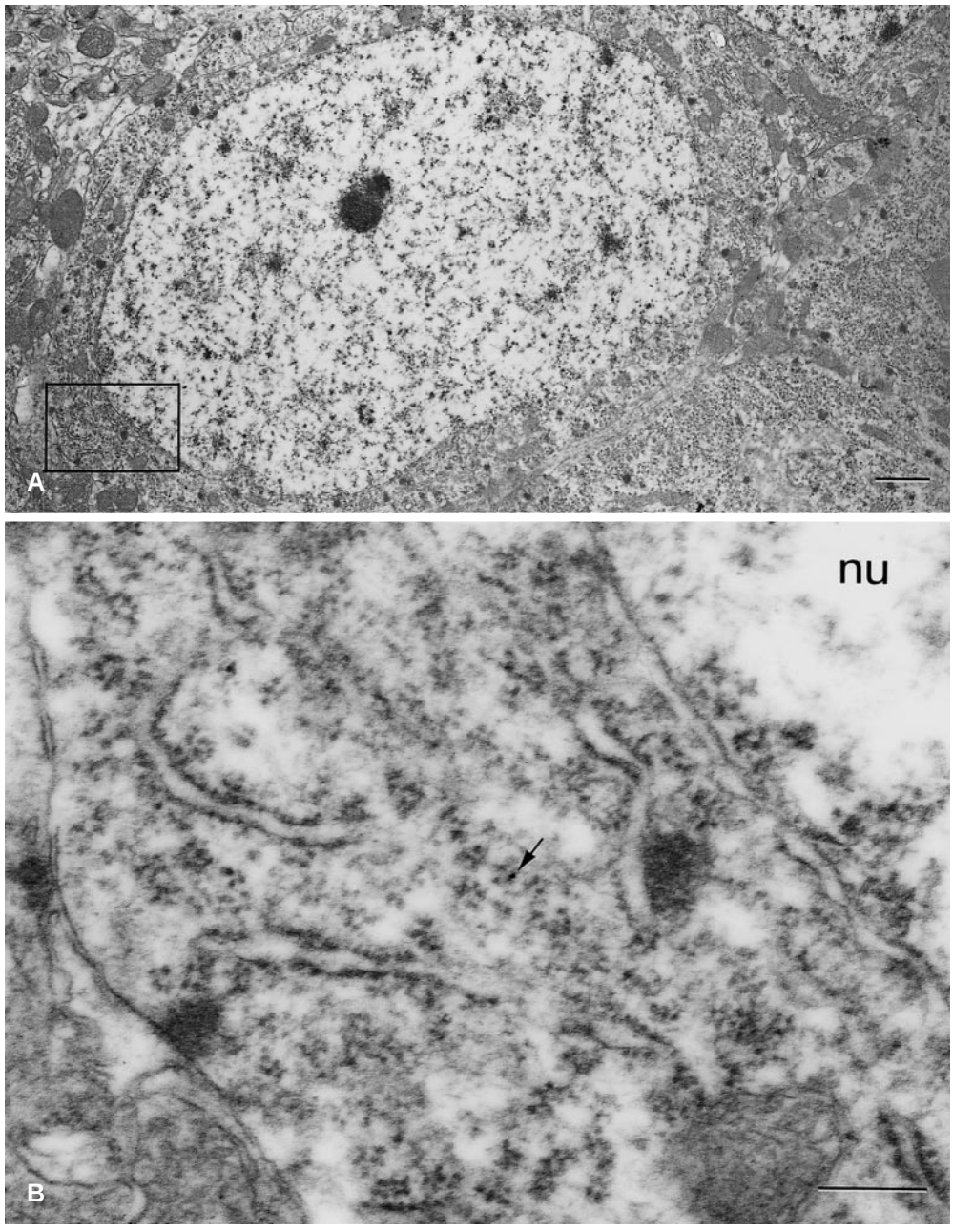

Fig. 4 **A** Electron micrograph of gold-conjugated eIF2α(P) immunostaining in a non-ischemic CA1 pyramidal neuron. *Outlined area* is reproduced at higher magnification in **B**. **B** Only one gold particle *(arrow)* is found in this portion of the cytoplasm, whereas the nucleus *(nu)* contains no gold particles. *Bar* **A** 1 μm B 200 nm

beling was found in sections when the eIF2α(P) antisera was preblocked with 55 nM antigenic peptide (Fig. 1 D). The most intensely labeled areas of dorsal hippocampus from reperfused brains occurred in the pyramidal cell body layer of the CA1 hippocampal sector (Fig. 1, arrows), and staining was also present in the CA3 sector, hilar region and granule cells of the dentate gyrus (Fig. 1 B, C). Faint labeling occurred in the dendritic layers throughout the hippocampus, and nonspecific staining in the alveus was attributed to chromogen affinity of myelinated fibers there.

Compartmentalization of eIF2α(P) after 10-min ischemia and 10-min reperfusion

Light microscopy

The bulk of eIF2α(P) immunostaining after 10-min ischemia/10-min reperfusion was confined to the cytoplasm of nerve cell perikarya and the initial portion of dendrites in the hippocampal areas mentioned above. Figure 2 shows such staining in the pyramidal cell layer of the CA1 sector (Fig. 2 A), as well as in the hilar region and adjacent granule cell layer of the ventral blade of dentate gyrus (photomontage Fig. 2 B). None of the light microscopic preparations at these magnifications showed neuronal eIF2α(P) nuclear labeling of CA1 pyramidal neurons;

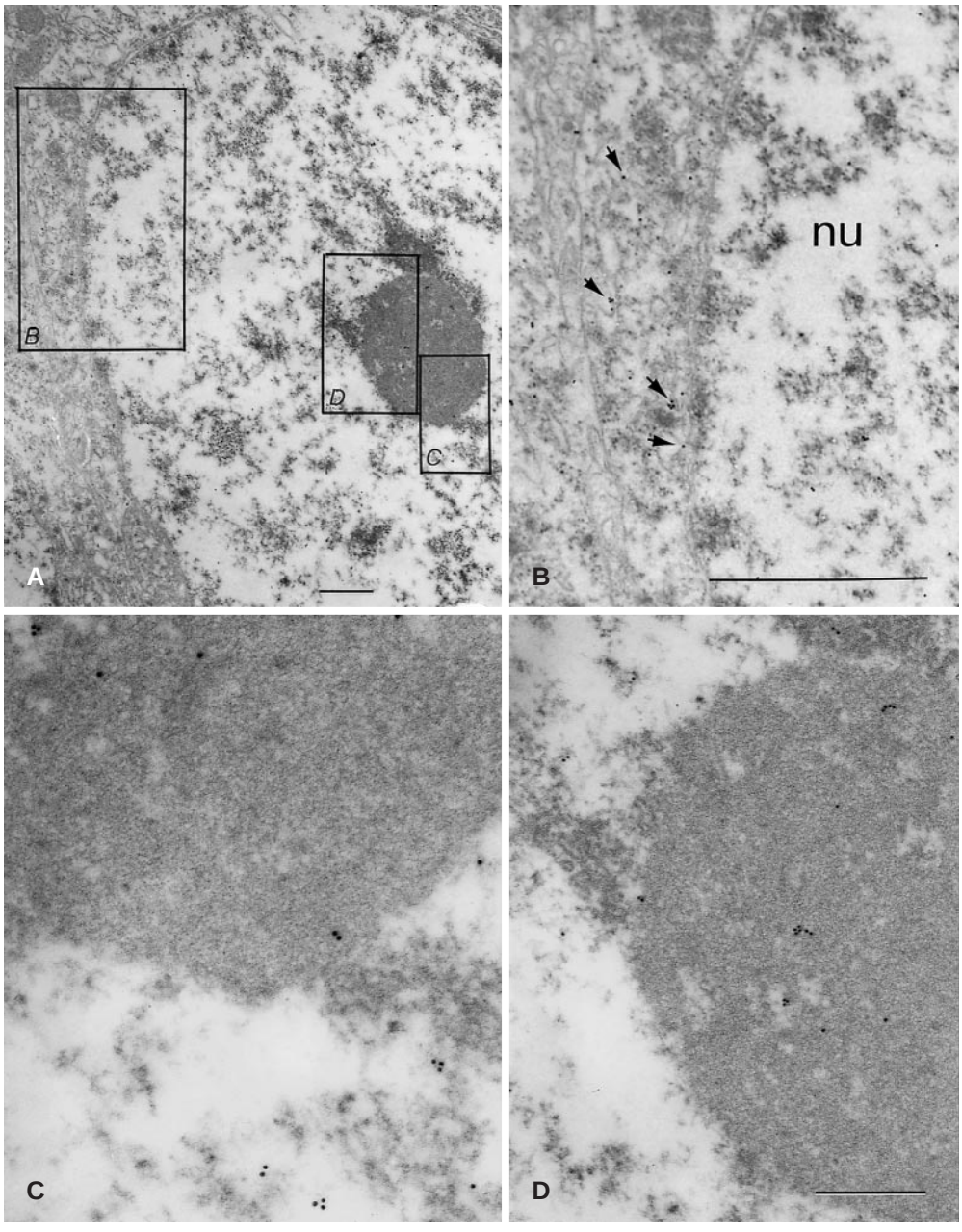

Fig. 5 **A** Electron micrograph of gold-conjugated eIF2α(P) immunostaining in a CA1 pyramidal neuron after 10-min ischemia and 10-min reperfusion. Areas *outlined by rectangles* are reproduced at higher magnification in **B, C** and **D**. **B** Nucleus *(nu)* and adjacent cytoplasm. Note numerous gold particles in cytoplasm *(arrows)*. **C, D** Nucleolus and adjacent nucleoplasm. Scattered gold particles indicate light staining in the nucleolus, adjacent nuclear chromatin, and nuclear matrix. *Bars* **A, B** 1 μm; **D** (also for **C**) 200 nm

however, some nuclear eIF2α(P) was revealed with electron microscopy (EM, see below). Moderate staining was also evident in putative glial cells and in endothelial cells that line hippocampal blood vessels (Fig. 2, arrows). At high magnification (× 2000) the localization of eIF2α(P) in the cytoplasm of CA1 neurons (Fig. 3 A), dentate granule cells (Fig. 3 C), and hilar cells (Fig. 3 D) was confirmed. In addition, intense labeling of nerve cells in the stratum oriens, radiatum, and lacunosum/moleculare suggests that varieties of hippocampal interneurons were affected by the same sequelae that affected pyramidal and granule cell neurons. An example of one such cell from the stratum oriens is shown in Fig. 3 B. At high magnification it was also possible to recognize lightly stained astrocytic cell bodies and their long, radiating processes (Fig. 3 E, arrow). Astrocytic foot processes were occasionally observed apposing the outer perimeter of hippocampal blood vessels, contributing to the perivascular sheath (Fig. 3 G, ap). Furthermore, the staining of glia was not confined only to astrocytes because some oligodendrocytes also showed moderate immunostaining in their cytoplasm (Fig. 3 F, arrow).

Electron microscopy

In contrast to ultrathin sections through the CA1 from non-ischemic brains, which showed little or no IG (Fig. 4), sections from brains after 10-min ischemia/10-min reperfusion showed distinct patterns of neuronal, glial,

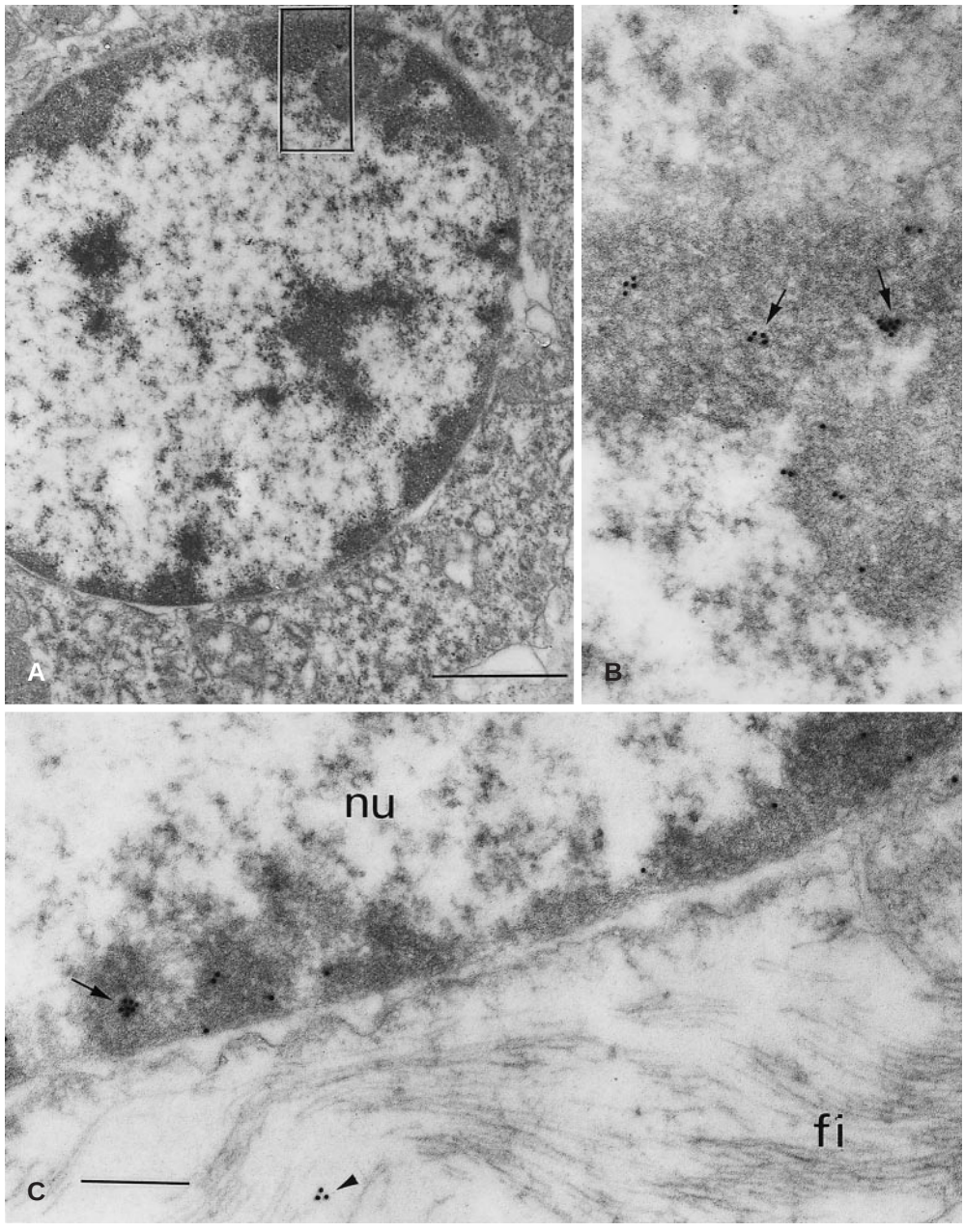

Fig. 6 A–C Electron micrographs of eIF2α(P) immunostained glia in the CA1 hippocampal sector after 10-min ischemia and 10-min reperfusion. *Area outlined by rectangle* in **A** is reproduced at a higher magnification in **B.** **A** Oligodendrocyte; **B** immunogold particles *(arrows)* indicate light staining of the nucleus of the oligodendrocyte; **C** portion of an astrocyte with light immunostaining of the nuclear chromatin *(arrow)* and the cytoplasm *(arrowhead)* (*fi* glial filaments). *Bars* **A** 1 μm; **C** (also for **B**) 200 nm

and endothelial subcellular eIF2α(P) localization. CA1 pyramidal neurons had moderate numbers of IG particles in the perikaryal cytoplasm (Fig. 5 A, B) and scattered particles distributed throughout the nucleus (Fig. 5 C, D). In the cytoplasm, although a few IG particles appeared to be free, they were mostly associated with the rough endoplasmic reticulum (RER) (Fig. 5 B, arrows). In the nucleus IG particles were associated with the: (1) nucleolus, (2) adjacent nuclear chromatin, and (3) nuclear matrix (Fig. 5 C, D). Further analyses of the glia localization revealed IG clusters associated with the nuclear chromatin of both oligodendrocytes (Fig. 6 A, B) and astrocytes (Fig. 6 C). In hippocampal blood vessels clusters of IG particles were found in association with the endothelial nuclear chromatin and the nuclear envelop, while scattered particles were also present in the cytoplasm of both endothelial cells and adjacent perivascular astrocytes (Fig. 7 A, 7 B).

Compartmentalization of eIF2α(P) after 10-min ischemia and 60-min reperfusion

Light microscopy

Although the pattern of eIF2α(P) immunostaining of the dorsal hippocampus after 10-min ischemia/60-min reperfusion resembled that after 10-min ischemia/10-min reperfusion, some notable differences were found. First, increased staining was evident in the perikaryal and dendritic cytoplasm of many hippocampal neurons. Apical

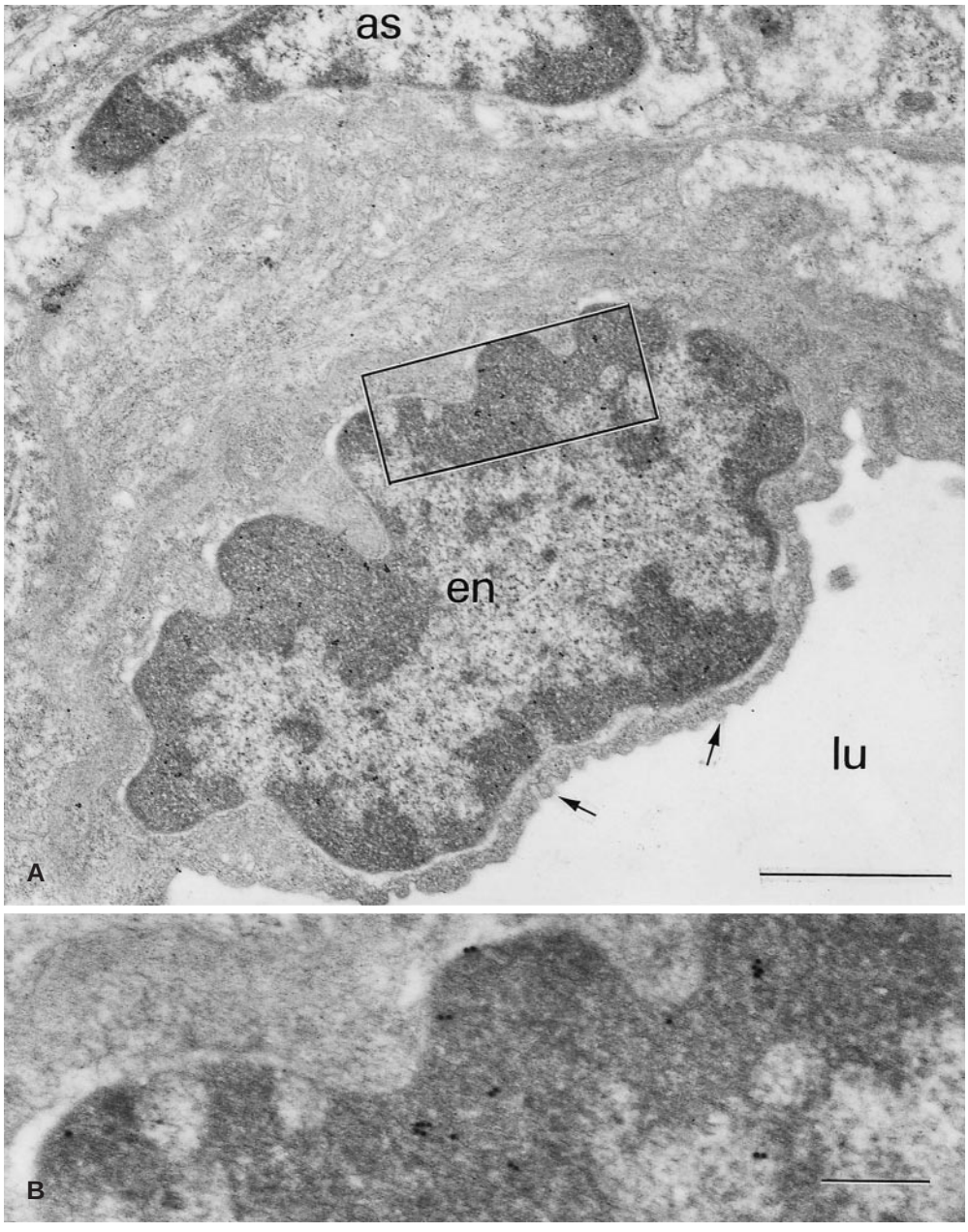

Fig. 7 A, B Electron micrographs of a CA1 microvessel from a 10-min ischemic 10-min reperfused brain after eIF2α(P)/immunogold staining. **A** Portions of the endothelium *(en)*, microvessel lumen *(lu)* and a perivascular astrocyte *(as)*. Note that the endothelial nucleus, as well as the luminal membrane *(arrows 3 are deeply folded, suggesting a state of contractility*. Area outlined by the *rectangle* is reproduced at a higher magnification in **B**. **B** Scattered gold particles are found in the nucleus and nuclear membrane. *Bars* **A** 1 μm, **B** 200 nm

dendrites of CA1 neurons were visualized extending from the pyramidal cell layer into the adjacent stratum radiatum (Fig. 8 A). Hilar cell dendrites could also be followed to their first and sometimes second branching points (Fig. 8 B). These findings suggested that eIF2α(P) was not only more pervasively distributed in the perikaryon but that eIF2α may also have undergone phosphorylation in distal regions of the processes, that are known to contain elements of the RER. However, these findings were not seen in all hippocampal neurons. In fact, dentate granule cells actually displayed lighter staining of the cell body as compared with that seen in the 10-min reperfused tissue (compare the dentate granule cell bodies in Figs. 2 B and 8 B). The second important finding in the 60-min reperfused tissue was the presence of light immunostaining in the nuclei of some hippocampal CA1 neurons, consistent with the previous observation of increased localization of eIF2α(P) in these nuclei with increasing time of reperfusion.

High-power (× 2000) light microscopic examination confirmed the findings in CA1 (Fig. 9 A) and hilar (Fig. 9 B) neurons, and also revealed the absence of staining in glia (Fig. 9 C) and endothelial cells (Fig. 9 D). In addition, the nuclei of some CA1 neurons appeared lightly labeled (Fig. 9 A).

Electron microscopy

EM analyses of ultrathin sections through the CA1 after 10-min ischemia/60-min reperfusion revealed qualitative

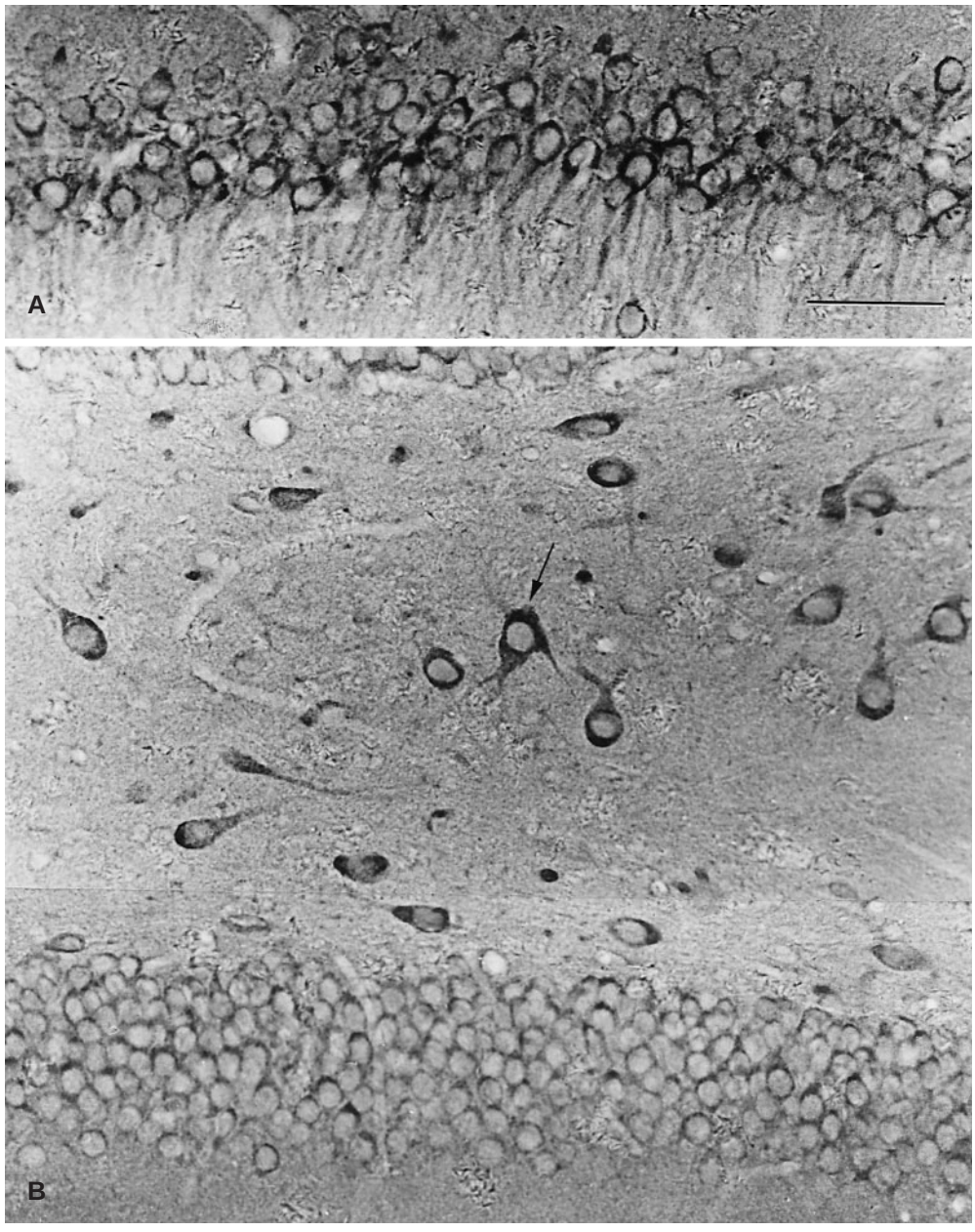

Fig. 8 A, B eIF2α(P) immunostaining in coronal sections of the dorsal hippocampus following 10-min ischemia and 60-min reperfusion. **A** In most CA1 pyramidal neurons deep cytoplasmic immunostaining extends into apical dendrites. **B** Photomontage includes the hilar region (*upper 2/3* of figure) and the ventral blade of the dentate gyrus. Deep staining of the cell bodies in hilar neurons extends into the dendrites. *Arrow* points at the hilar cell shown at higher magnification in Fig. 9 B. Also note lighter staining of the dentate granule cells as compared to that in Fig. 2 B. *Bar* **A** 50 μm

increases of eIF2α(P) in pyramidal neurons compared with those found at 10 min of reperfusion. Such increases were noted in both the cytoplasm (Fig. 10 A, B) and the nucleus (Fig. 11 A, B). High-resolution analyses revealed eIF2α(P) in discrete subcellular compartments in both cytoplasm and nucleus. In the cytoplasm IG particles were localized primarily to the: (1) outer aspect of the nuclear envelope, (2) RER, and (3) outer membrane of mitochondria (Fig. 10 B, single arrow, double arrows, and arrowheads, respectively). In the RER many IG particles aligned themselves along the membrane of the cisterna. Scattered particles were also found throughout the cytosol with no apparent relationship to any organelle and could represent eIF2/eIF2B complexes dissociated from ribosomes. In the nucleus, IG particles were found predominately associated with three structures: (1) peripheral areas of the nucleolus, (2) nuclear chromatin strands, and (3) thin, putative nuclear filaments (Fig. 11, single arrow, double arrows). No IG particles were found in relation to any glial cell type or vascular endothelium (data not shown).

Discussion

Here we: (1) reconfirmed the temporal and cellular localization of eIF2α(P) within SVNs of the rat hippocampus, (2) observed eIF2α(P) immunostaining in endothelial cells and glia after 10- but not after 60-min reperfusion, and (3) for the first time characterized the ultrastructural localization of eIF2α(P) within CA1 neurons after 10-min ischemia followed by either 10-min or 1-h reperfusion.

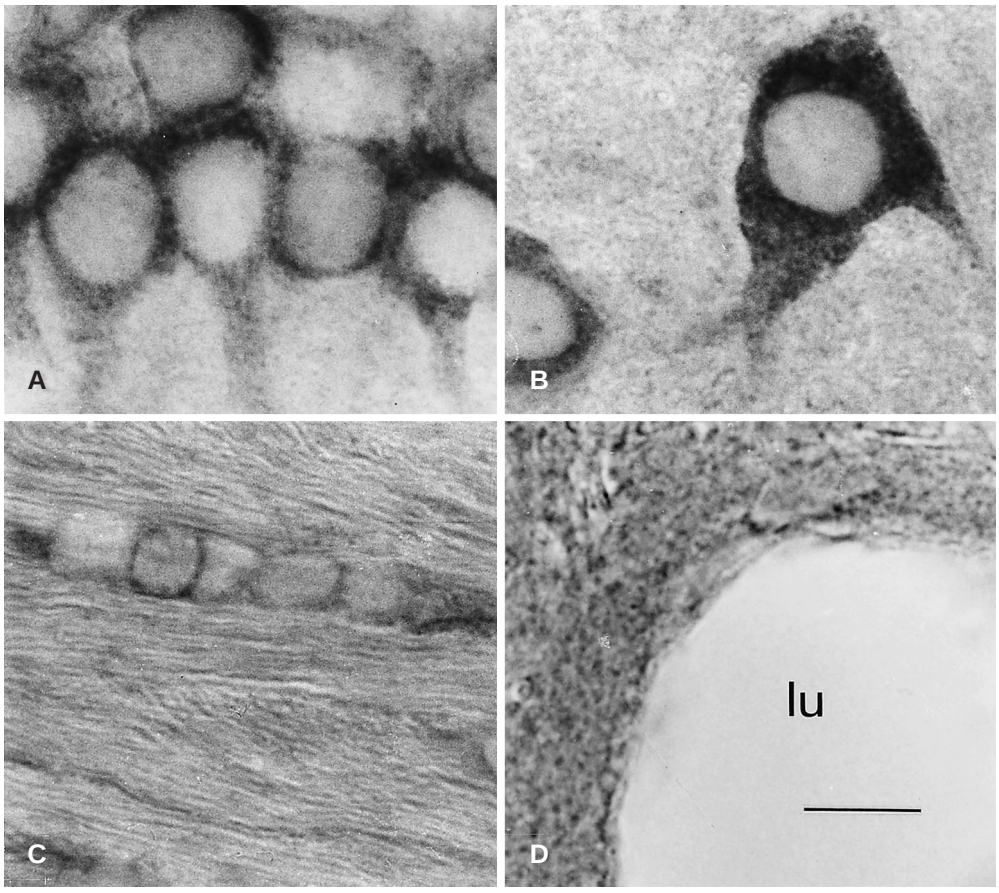

Fig. 9 A–D Higher-power photomicrographs of eIF2α(P) immunostaining following 10-min ischemia and 60-min reperfusion. **A** CA1 pyramidal neurons. Note that a few of the pyramidal cell nuclei appear lightly labeled. **B** Hilar neuron. **C** Immunostaining is now absent from interfascicular oligodendrocytes in the corpus callosum and **D** from endothelial cells and apposed astrocytic foot processes. *Bar* **D** 10 μm

eIF2α(P) and selective neuron vulnerability

The fact that the brain's response to ischemia and reperfusion is not regionally homogeneous in the dorsal hippocampus is evident when immunostaining in the CA1 and dentate gyrus are compared. Whereas the light-level immunolabeling of the dentate gyrus (a non-vulnerable area) diminishes substantially after 60 min of reperfusion, it intensifies in the CA1, and this is also seen at the ultrastructural level. As expected from the role of eIF2α in regulating translation initiation, accumulation of eIF2α(P) co-maps with reduced protein synthesis during reperfusion [21], and here eIF2α(P) is ultrastructurally associated with ribosomes along the RER in CA1 pyramidal neurons. Furthermore, the neurons most susceptible to delayed neuronal death (i.e., CA1 and some hilar cells) after ischemia are those that do not regain normal protein synthesis [14], and emerging evidence suggests that apoptosis of these cells could be triggered by eIF2α(P) itself [8, 19].

eIF2α(P) nuclear compartmentalization

In our previous light-level characterization of the localization of eIF2α(P) during reperfusion [4], we observed nuclear localization of eIF2α(P) in CA1 neurons by 60 min of reperfusion. The ultrastructural studies here confirm this finding, although in the present study light-level nuclear immunostaining is less evident. Our earlier light microscopic studies were done using methanol/acetic acid fixation, which does not cross-link proteins and more readily allows antibody penetration of the tissue, yet is not adequate for ultrastructural study. Unlike other fixatives, it is known that aldehydes form both intramolecular and intermolecular cross-links with protein molecules, resulting in the formation of more rigid heteropolymers [7]. Here, although the aldehyde fixation provided good structural preservation for EM analysis, it reduced immunostaining of eIF2α(P) and required antigen-retrieval procedures [1] to achieve light-level cytoplasmic immunostaining. Thus, nuclear penetration by the antibody in the 30-μm sections was apparently poor. As evidenced by the IG preparations, the failure of the antibody to immunostain nuclei at the light level did not necessarily reflect the absence of the antigen, but rather was due to the inability of the antibody to reach the protein in the nucleus under the conditions used to prepare and incubate the material [1].

Lobo et al. [10], utilizing ultrastructural techniques and an antibody that did not discriminate between phosphorylated and unphosphorylated eIF2α, observed eIF2α within nuclei of cultured neurons that had not sustained any insult. The fact that we have never observed eIF2α(P) in nuclei of uninjured neurons argues that the nuclear isoform of eIF2α observed by Lobo et al. was unphosphorylated. However, after 60-min reperfusion we have observed abundant eIF2α(P) in the nuclei of vulnerable CA1

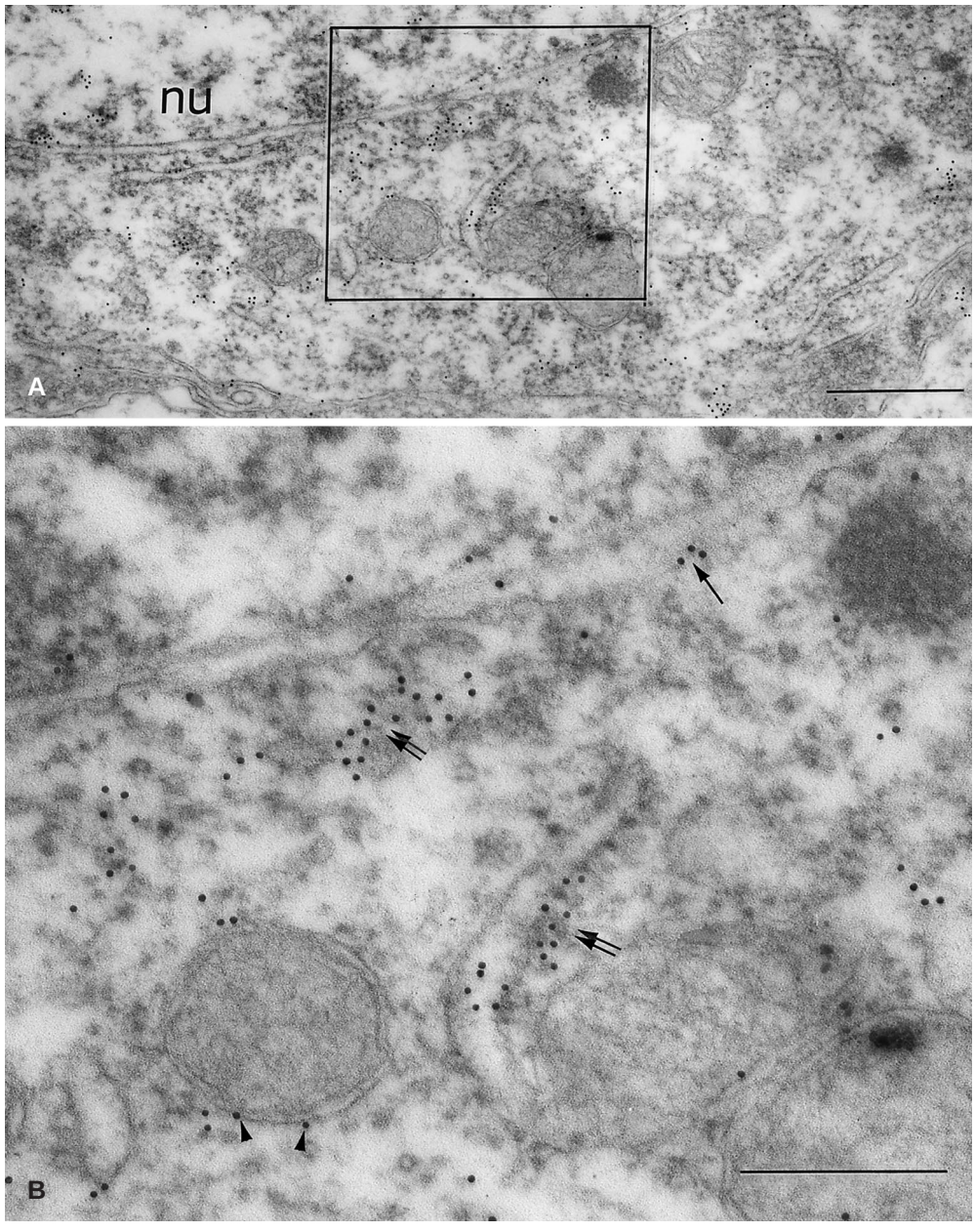

Fig. 10 **A** Electron micrograph of gold-conjugated eIF2α(P) immunostaining in a CA1 pyramidal neuron after 10-min ischemia and 60-min reperfusion shows portions of the nucleus *(nu)* and cytoplasm. The *outlined area* reproduced at a higher magnification in **B** shows immunogold localization: (1) at the nuclear envelop *(arrow)*, (2) on the rough endoplasmic reticulum *(double arrows)*, and (3) on the outer mitochondrial membrane *(arrowheads)*. *Bars* **A** 1μm, **B** 250 nm

neurons, both at the light level in methanol/acetic acid-fixed sections [4] and at the EM level in aldehyde-fixed tissue. The α-subunit of eIF2 contains in its primary sequence several nuclear localization signals, such as RRRIR (52-56), KRR (86-88), or KYKR (140-143) [5, 15]. In particular, the RRRIR site is immediately adjacent to the Ser^{15} phosphorylation site and could become exposed by the hydrophilic effect of the phosphorylation. Indeed, in CA1 neurons at 1-h reperfusion, ultrastructural localization of eIF2α(P) revealed numerous gold particles within peripheral areas of the nucleolus, on nuclear chromatin strands, and along putative nuclear filaments. Whether these localizations represent true binding of eIF2α(P) to ultrastructural nuclear components remains unclear. However, electromobility shift assays, to assess the DNA binding capability of eIF2α(P), are currently underway in our laboratory to resolve this issue. It is also known that the β-subunit of eIF2 contains nucleotide binding motifs that are not involved in binding GTP or Met-tRNA (reviewed in [3]). Our observations, together with those of Lobo et al. [10], and the emerging evidence directly implicating eIF2α(P) in induction of apoptosis raise important fundamental questions regarding potential nuclear functions of α-subunit-phosphorylated eIF2.

eIF2α(P) presence in non-neuronal cells

Although not our primary aim, our data also revealed cellular staining of both glia (astrocytes and oligodendrocytes) and endothelial cells within the dorsal hippocampus. Unlike our previous study [4], no astrocytic staining

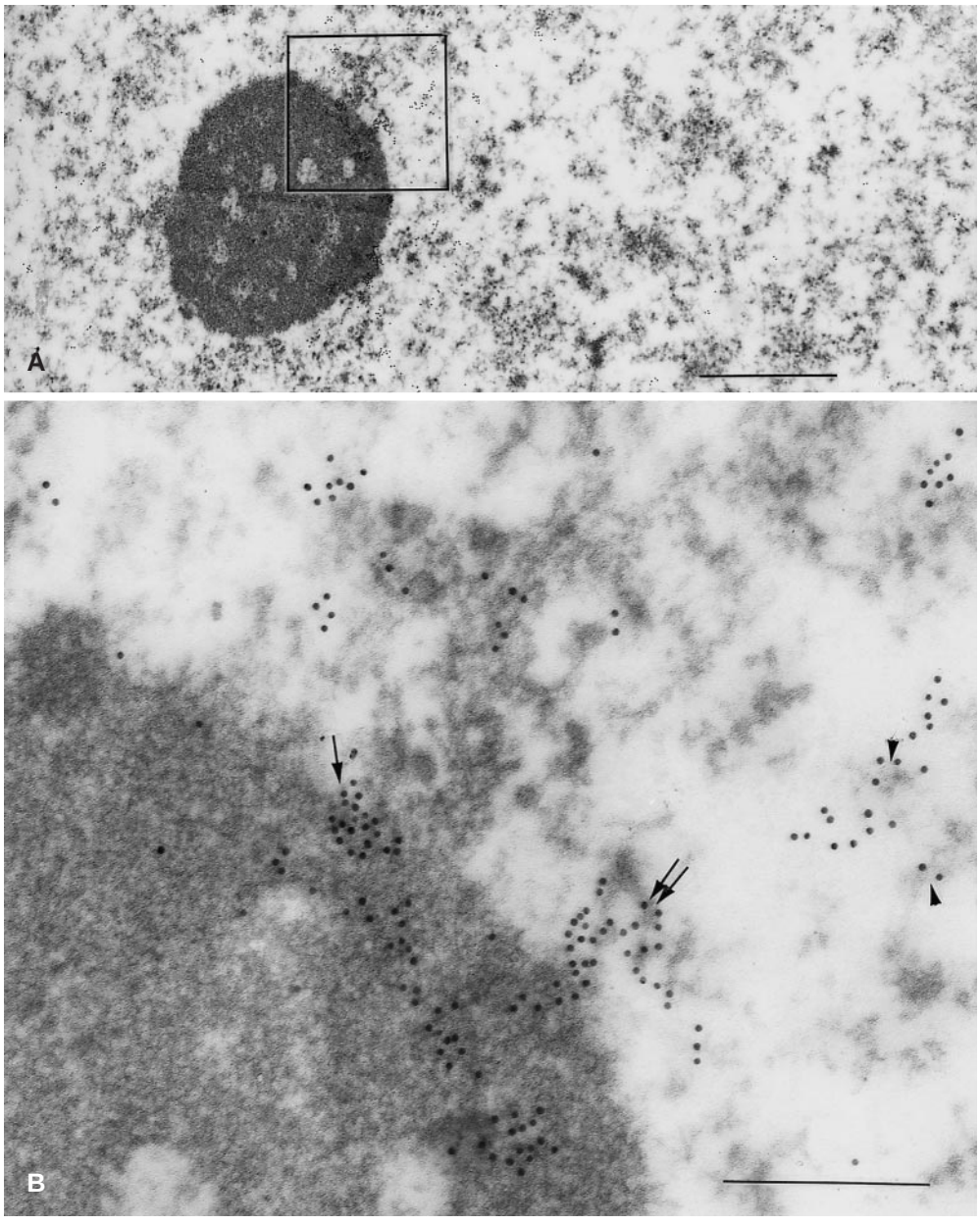

Fig. 11 **A** Electron micrograph of gold-conjugated eIF2α(P) immunostaining in a CA1 pyramidal neuron after 10-min ischemia and 60-min reperfusion shows the nucleolus and adjacent nucleoplasm. Numerous gold particles are scattered throughout the peripheral nucleolus and the nucleoplasm. **B** Higher magnification of *area outlined* in **A** shows gold particles: (1) in the peripheral areas of the nucleolus *(arrow)*, (2) on nuclear chromatin strands *(double arrows)* and (3) on thin nuclear filaments *(arrowheads)*. *Bars* **A** 1 μm, **B** 250 nm

was observed in the non-ischemic control brains, but it is likely that the major modification in fixation procedure affected this observational difference. In addition, this earlier investigation [4] showed a lack of eIF2α(P) staining in astrocytes from the ischemic, non-reperfused brains. Our current study did, however, resolve identifiable glial staining after 10 min of reperfusion that was absent by 60 min of reperfusion. Light microscopy revealed cytoplasmic glial staining, while subcellular observations found a few IG particles associated with nuclear chromatin in astrocytes and oligodendrocytes. The IG particle density we observed in glial nuclei never approached the IG density seen in the nuclei of vulnerable neurons at 60-min reperfusion, and recognition of this difference is consistent with our earlier observations [4]. Tissue subjected to 60 min of reperfusion displayed no detectable glial staining in either this or our previous study [4]. While light staining of glial cells may signal diminished capacity for protein synthesis during early reperfusion, the loss of eIF2α(P) staining that we observed within these cells may actually reflect enhanced protein synthesis during later reperfusion [13].

The novel discovery of eIF2α(P) immunostaining within the endothelial cells lining hippocampal blood vessels was also unexpected. However, it is known that during post-ischemic reperfusion endothelial cells generate nitric oxide, and there is recent evidence showing that elevated levels of nitric oxide induce phosphorylation of eIF2α [9]. After 10 min of reperfusion, both cytoplasmic and nuclear labeling is evident, and some anti-eIF2α(P)-conjugated IG particles are associated with nuclear chromatin. As was the case for glia, endothelial cells are also devoid of immunostaining after 60 min of reperfusion.

These findings suggest that following 10-min ischemia non-neuronal cells may effectively deal with mechanisms leading to reperfusion-induced injury.

The exact mechanisms by which glia and endothelial cells resist injury by ischemia and reperfusion are unknown, but they evidently rapidly dephosphorylate eIF2α(P) and do not sustain prolonged inhibition of protein synthesis. In contrast, vulnerable neurons do sustain prolonged inhibition of protein synthesis, associated with persistent cytosolic eIF2α(P) and accumulation of substantial amounts of nuclear eIF2α(P).

Summary and conclusions

The results from this study provide morphological evidence supporting both cytosolic and nuclear roles for eIF2α(P) after reperfusion. Given the evidence that eIF2α(P) itself induces apoptosis [19], it is clear that further studies must examine the question of whether eIF2α(P) has important implications for regulation of transcription or post-transcriptional processing as well as for regulation of translation initiation during brain reperfusion.

Acknowledgements This project was supported in part by the National Institute of Health Grant NS33196. The authors thank Jonathon M. Sullivan, Donald J. DeGracia, and Gary S. Krause for their technical and editorial support of this investigation.

References

1. Brown D, Lydon J, McLaughlin M, Stuart-Tilley A, Tyzkowski R, Alper S (1996) Antigen retrieval in cryostat tissue sections and cultured cells by treatment with sodium dodecyl sulfate (SDS). Histochem Cell Biol 105 : 261–267
2. Cohen P (1989) The structure and regulation of protein phosphatases. Annu Rev Biochem 58 : 453–508
3. DeGracia DJ, Neumar RW, White BC, Krause GS (1996) Global brain ischemia and reperfusion: modification in eukaryotic initiation factors are associated with inhibition of translation initiation. J Neurochem 67 : 2005–2012
4. DeGracia DJ, Sullivan JM, Neumar RW, Alousi SS, Hikade KR, Pittman JE, White BC, Rafols JA, Krause GS (1997) Effect of brain ischemia and reperfusion on the localization of phosphorylated eukaryotic initiation factor 2α. J Cereb Blood Flow Metab 17 : 1291–1302
5. Earnst H, Duncan RF, Hershey JWB (1987) Cloning and sequencing of complementary DNAs encoding the α subunit of translation initiation factor eIF-2. J Biol Chem 262 : 1206–1212
6. Farrell PJ, Balkow K, Hunt T, Jackson RJ, Trachesl H (1977) Phosphorylation of initiation factor eIF-2 and the control of reticulocyte protein synthesis. Cell 11 : 187–200
7. Hayat MA (1989) Principles and techniques of electron microscopy: biological applications, 3rd edn. CRC Press, Boca Raton, p 25
8. Kaufman RJ, Kuymar KU, Wu S, Srivastava SP (1998) Regulation of the double-stranded RNA-dependent protein kinase (PKR) and its role in apoptosis. Translational Control. Cold Spring Harbor Laboratory Press, Cold Spring Harbor, p 330
9. Kim YM, Son K, Hong SJ, Green A, Chen JJ, Tzeng E, Hierholzer C, Billiar TR (1998) Inhibition of protein synthesis by nitric oxide correlates with cytostatic activity: nitric oxide induces phosphorylation of initiation factor eIF-2α. Mol Med 4 : 179–190
10. Lobo MVT, Alonso FJM, Rodriguez S, Alcazar A, Martin E, G-Santander R, Salinas M, Fando JL (1997) Localization of eukaryotic initiation factor 2 in neuron primary cultures and established cell lines. Histochem J 29 : 453–468
11. Merrick W (1992) Mechanism and regulation of eukaryotic protein synthesis. Microbiol Rev 56 : 291–315
12. Nowak TS Jr, Fried RL, Lust WD, Passonneau JV (1985) Changes in brain energy metabolism and protein synthesis following transient ischemia in the gerbil. J Neurochem 44 : 487–494
13. Oosteveen JA, Dunn E, Carter DB, Hall ED (1998) Neuroprotective efficacy and mechanisms of novel pyrrolopyromidine lipid peroxidation inhibitors in the gerbil forebrain ischemia model. J Cereb Blood Flow Metab 18 : 539–547
14. Pulsinelli W, Brierley J, Plum F (1982) Temporal profile of neuronal damage in a model of transient forebrain ischemia. Ann Neurol 11 : 491–489
15. Qu S, Cavener DR (1994) Isolation and characterization of the *Drosophila Melanogaster* eIF-2α gene encoding the alpha subunit of translation initiation factor eIF-2. Gene 140 : 239–242
16. Redpath NT, Proud CG (1994) Molecular mechanisms in the control of translation by hormones and growth factors. Biochim Biophys Acta 1220 : 147–162
17. Rowlands AG, Panniers R, Henshaw E (1998) The catalytic mechanism of guanine nucleotide exchange factor action and competitive inhibition by phosphorylated eukaryotic initiation factor 2. J Biol Chem 263 : 5526–5533
18. Samuel CE (1993) The eIF2α protein kinases, regulators of translation from yeasts to humans. J Biol Chem 268 : 7603–7606
19. Srivastava SP, Kumar KU, Kaufman RJ (1998) Phosphorylation of eukaryotic translation initiation factor 2 mediates apoptosis in response to activation on the double-stranded RNA-dependent protein kinase. J Biol Chem 273 : 2416–2423
20. Stirling JW, Graff PS (1995) Antigen unmasking for immunoelectron microscopy: labeling is improved by treating with sodium ethoxide or sodium metaperiodate, the heating on retrieval medium. J Histochem Cytochem 43 : 115–123
21. Sullivan JM, DeGracia DJ, Rafols JA, White BC (1998) Insulin induces dephosphorylation of eIF2α(P) and recovery of protein synthesis in selectively vulnerable hippocampal neurons during reperfusion. Translational Control. Cold Spring Harbor Laboratory Press, Cold Spring Harbor, p 261
22. Widmann R, Kuroiwa T, Bonnekoh D, Hossmann KA (1991) [^{14}C]Leucine incorporation into brain proteins in gerbils after transient ischemia: relationship to selective vulnerability of hippocampus. J Neurochem 56 : 789–796